Quantitative Analysis of Long-Range Interactions between Adsorbed Dipolar Molecules on Cu(111)

Takashi Yokoyama,* Tomonori Takahashi, and Kazuteru Shinozaki
International Graduate School of Arts and Sciences, Yokohama City University, 22-2 Seto, Kanazawa-ku, Yokohama 236-0027, Japan

Masakuni Okamoto
Mechanical Engineering Research Laboratory, Hitachi Limited, 832-2 Horiguchi, Hitachinaka, Ibaraki 312-0034, Japan
(Received 27 February 2007; published 14 May 2007)

Highly dispersed superstructures of a dipolar iridium complex are formed on a Cu(111) surface. We show that the dilute superstructures with density-controlled intermolecular separations are stabilized by the strong and long-range repulsive intermolecular interactions. The repulsive intermolecular interactions are quantitatively evaluated by using low-temperature scanning tunneling microscopy, which are characterized by the surface-enhanced dipole-dipole interactions.

DOI: 10.1103/PhysRevLett.98.206102 PACS numbers: 68.43.Hn, 68.37.Ef, 68.43.Jk

The controlled positioning and assembling of functional molecules on surfaces are currently attracting considerable interest [1,2]. Recently, a rich variety of molecular nanostructures such as clusters, wires, and extended networks has been selectively assembled on surfaces [3–6], which has been directly characterized by scanning tunneling microscopy (STM). In this approach, the selective molecular assembly has been controlled by tuning directional intermolecular attractions such as hydrogen bondings [7]. In contrast to such an attractive interaction, repulsive intermolecular interactions should play also a significant role in the molecular assembly. Silly *et al.* [8] created well-ordered atomic superlattices on a Ag(111) surface, in which hexagonal arrays of Ce adatoms with a 3.2 nm periodicity are stabilized by the interactions of surface-state electrons with Ce adatoms. Although the atomic superlattices were stable only at a low temperature of 3.9 K, Lukas *et al.* [9] have found that regular molecular stripes of one-dimensional pentancene rows on a Cu(110) surface, achieved by a substrate-mediated inter-row repulsion, are stable for temperatures up to 450 K. Since the stability of the superstructures is associated with the interaction potentials between adsorbates, a quantitative understanding of adsorbate-adsorbate interactions and the influence of substrates should be required to control molecular self-assembly [10,11].

In this Letter, we report strong and long-range repulsive interactions between dipolar molecules on a Cu(111) surface which lead to the formation of highly dispersed molecular superstructures with density-controlled intermolecular spacings. STM observations reveal that individual adsorbed molecules are separately distributed on the surface. To evaluate the intermolecular interactions quantitatively, we measure the nearest-neighbor separations r between adsorbed molecules, and the obtained intermolecular potential is consistent with the dipole-dipole interactions with a decay as r^{-3}. Nevertheless, the obtained repulsive interactions are considerably stronger than that expected from the permanent dipole moment of the molecule.

We have used a facial cyclometalated complex of tris-(2-phenylpyridine)iridium(III), fac-Ir(ppy)$_3$ [12], in which the three phenylpyridine (ppy) ligands surrounding an Ir ion exhibit a propeller-shaped conformation [13,14] with an inherent C_3 symmetry as shown in Fig. 1. Because of its very high efficiency of electrophosphorescence, Ir(ppy)$_3$ has been widely used as a luminescent material in the organic light-emitting devices [15,16]. In addition, a quite large dipole moment of 6.5 D along the C_3 axis has been calculated for fac-Ir(ppy)$_3$ [14], which results from charge transfer from the central Ir ion to the phenyl moieties of the ppy ligands. To investigate intermolecular interactions of adsorbed Ir(ppy)$_3$ on Cu(111), we used a low-temperature STM operated under ultrahigh vacuum (UHV) conditions. Electrochemically etched W tips were used for the STM probe. The Cu(111) substrate was prepared by repeated cycles of Ar^+ sputtering and annealing in a UHV chamber to obtain atomically flat surface without impurities. The Ir(ppy)$_3$ molecules were thermally evaporated at 473 K from a carefully outgassed Knudsen cell under UHV con-

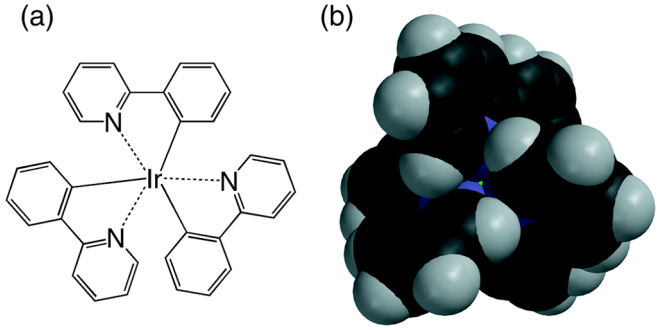

FIG. 1 (color online). (a) Chemical structure and (b) space filling model of fac-Ir(ppy)$_3$.

ditions. The Cu(111) sample was maintained at room temperature during the deposition and was subsequently transferred to the cooled microscope stage. All STM images were obtained in a constant-current mode at 81 K.

Figure 2(a) shows an STM image of the Cu(111) surface after a small amount of $Ir(ppy)_3$ was deposited. In the STM image, individual molecules appear as bright protrusions with about 0.25 nm height. Whereas they are preferentially adsorbed at step edges, isolated $Ir(ppy)_3$ monomers are randomly distributed on terraces. In a high-resolution STM image of Fig. 2(b), the single molecules are composed of three protrusions with a triangular configuration, in which each distance is estimated to be about 0.5 nm. On the basis of the molecular dimensions, each protrusion can be assigned as one of the ppy ligands, and the appearance of the three ppy ligands suggests that the C_3 symmetry axis of $Ir(ppy)_3$ is oriented perpendicular to the surface plane [see Fig. 1(b)]. Although the substrate-molecule interactions appear to be rather strong, we occasionally observed molecular hopping on terraces during slow STM imaging (>600 sec/image). The hopping rate derived from STM images was 0.014 ± 0.001 sec^{-1} at 81 K, almost independent of the tunneling parameter at around 50 pA. This result ensures that the adsorbed molecules are distributed on terraces under sufficient thermal equilibrium at 81 K,

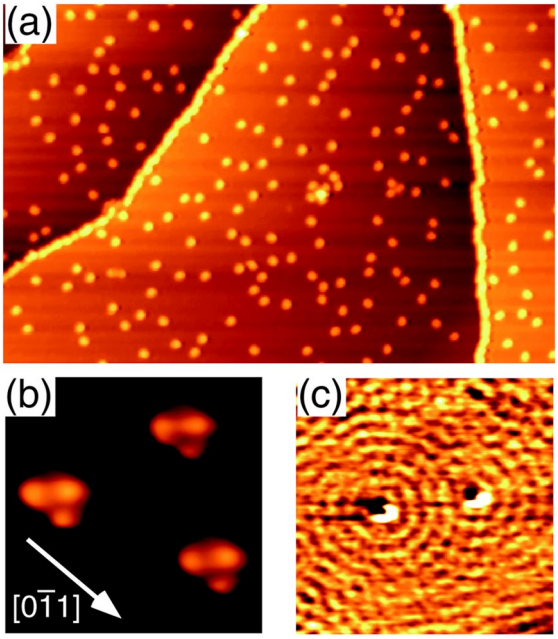

FIG. 2 (color online). (a) STM image of randomly distributed $Ir(ppy)_3$ molecules on Cu(111) obtained at 81 K (65 nm × 100 nm, sample voltage $V_s = 0.6$ V, and tunneling current $I_t = 80$ pA). The molecular density Θ is 0.028 nm^{-2}. (b) High-resolution STM image of $Ir(ppy)_3$ on Cu(111) at 81 K (4.0 nm × 4.0 nm, $V_s = -1.3$ V, and $I_t = 40$ pA). Each molecule is composed of three bright protrusions. (c) dI/dV STM image of circular standing-wave patterns around isolated two $Ir(ppy)_3$ molecules on Cu(111) at 81 K (25.0 nm × 25.0 nm, $V_s = -0.07$ V, and $I_t = 100$ pA).

and thus the distribution should be associated with the intermolecular interactions.

It has been reported that lateral interactions between metal adsorbates are mediated by the two-dimensional electron gas in Shockley-type surface states of Cu(111) [17,18]. Because of scattering surface-state electrons at adsorbates, the charge density oscillations are induced, which give rise to periodic electronic potentials called as the surface Friedel oscillations. The indirect interactions have a period of half of the Fermi wavelength with a decay as r^{-2}. In the present system, we find that $Ir(ppy)_3$ also acts as a scattering center. Figure 2(c) shows a differential-conductance (dI/dV) STM image at 81 K of isolated $Ir(ppy)_3$ molecules at a low bias voltage of -0.07 V, in which the circular standing-wave patterns appear around $Ir(ppy)_3$. The measured wavelength of about 1.5 nm is equivalent to the half of the Fermi wavelength of the surface states. Assuming the molecule to be a circular hard wall potential, the radius a of the effective potential for the surface-state electrons is estimated to be 0.13 ± 0.03 nm, which is much smaller than the molecular radius of about 0.5 nm. In the theory of Hyldgaard and Persson [19], the surface-state mediated interaction potential $E_{\text{int}}(r)$ is given by

$$E_{\text{int}}(r) \cong -AE_0\left(\frac{2\sin\delta_0}{\pi}\right)^2 \frac{\sin(2k_F(r-2a)+2\delta_0)}{[k_F(r-2a)]^2},$$

where A is a scattering amplitude, E_0 is the surface-state band edge, k_F is the Fermi surface wave vector, and δ_0 is the scattering phase shift. This periodic potential predicts the local energy minima at $r = 1.25$, 2.75, and 4.25 nm with a r^{-2} envelope, which leads to large populations at around these separations in the probability pair distributions. In terms of two-body interactions, the probability distribution $f_{\text{calc}}(r)$ modified by the intermolecular potential $E(r)$ can be estimated from $f_{\text{calc}}(r) = f_{\text{ran}}(r) \times \exp[-E(r)/k_BT]$ [18], where r is the nearest-neighbor separations between adsorbates, $f_{\text{ran}}(r)$ is the random separation distribution [20], and k_B is the Boltzmann constant. To clarify the influence of the surface Friedel oscillations, we measured the nearest-neighbor separations between adsorbed $Ir(ppy)_3$ molecules on Cu(111) at $T = 81$ K as a function of the molecular densities. Figure 3 shows the experimental probability distribution histograms $f(r)$ of the nearest-neighbor separations, measured from a total of 2019–4184 molecules (20–70 STM images) at each density. At a dilute density of 0.02 nm^{-2} in Fig. 3(a), the peak at $r = 2.59$ nm is almost consistent with the second peak at $r = 2.75$ nm of the calculated probability distributions (solid curve) $f_{\text{cal}}(r)$ associated with $E_{\text{int}}(r)$. The corresponding molecular pairs with the about 2.6 nm separations are highlighted by circles in the STM image of Fig. 3(a). We also observed the weak peak at $r \approx 2.6$ nm in other histograms at low molecular densities less than about 0.07 nm^{-2} (not shown), which indicates the intermolecular interactions are weakly affected by the surface Friedel

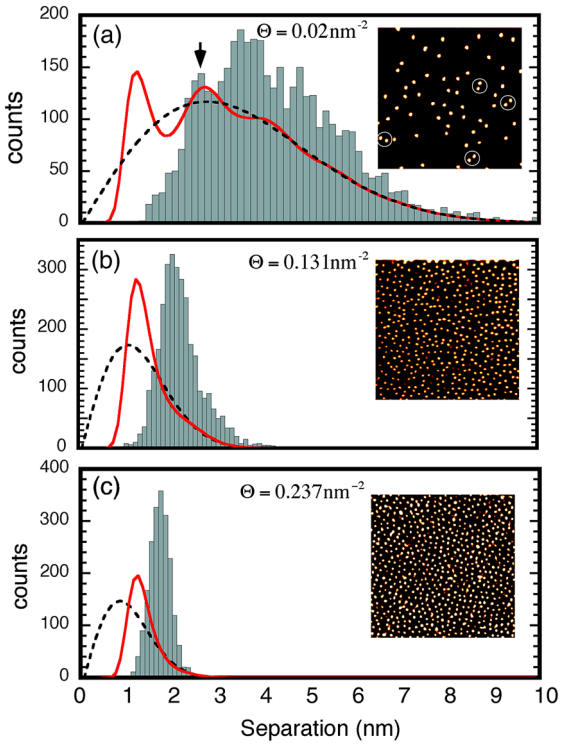

FIG. 3 (color online). Histograms of the nearest-neighbor separations of adsorbed Ir(ppy)$_3$ molecules on Cu(111) at molecular densities of (a) $\Theta = 0.020$ nm^{-2}, (b) 0.131 nm^{-2}, and (c) 0.237 nm^{-2}, measured from STM images at 81 K. The insets show typical STM images at each density (51.0 nm $\times$ 51.0 nm). The dotted curves display the random separation distribution $f_{\mathrm{ran}}(r)$ [20], and the red solid curves display the calculated probability distributions $f_{\mathrm{calc}}(r)$ modified by the surface Friedel oscillations $E_{\mathrm{int}}(r)$. In $E_{\mathrm{int}}(r)$, we have used a phase shift $\delta_0 = \pi/2$ for the hard wall potential and a typical scattering amplitude $A = 0.13$ used for a metal adsorbate [18].

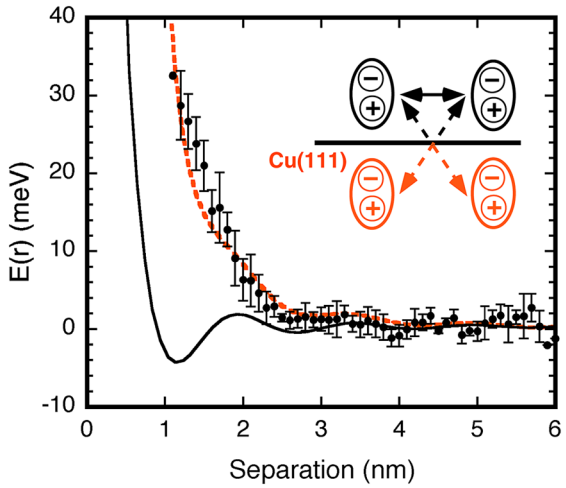

FIG. 4 (color online). Potential energy between two Ir(ppy)$_3$ molecules, evaluated from histograms of nearest-neighbor separations at six molecular densities ($\Theta = 0.020$, 0.028, 0.058, 0.068, 0.105, 0.131 nm^{-2}). The standard deviation of the mean is shown as the error bar. The solid curve shows the surface-mediated interaction potential $E_{\mathrm{int}}(r)$, originated from scattering surface-state electrons at Ir(ppy)$_3$. The orange dotted curve displays the calculated interaction potential fitted by including the dipole-dipole interaction ($\mu = 6.49$ D), dipole-mirror dipole interactions, and $E_{\mathrm{int}}(r)$. The inset shows the schematic illustration of intermolecular dipole-dipole and dipole-image dipole interactions.

oscillations. However, other experimental peaks cannot be reproduced, and the overall distributions are shifted to larger separations with respect to the calculated distributions. In addition, the deviation from the calculated distributions $f_{\mathrm{cal}}(r)$ becomes significant with increasing molecular density, as shown in Fig. 3. These results suggest that additional repulsive potentials are incorporated in this system.

To clarify the strong repulsive interactions, we have directly evaluated the interaction potential from $E(r) = -k_B T \ln[f(r)/f_{\mathrm{ran}}(r)]$, where $f(r)$ is the experimental histogram . Figure 4 shows the averaged potential curve obtained from six dilute densities ($\Theta = 0.020$, 0.028, 0.058, 0.068, 0.105, 0.131 nm^{-2})[21], in which the repulsive energy is much larger than the expected surface Friedel oscillations (solid curve) at $r < 2$ nm. By careful comparison with several kinds of decay functions, we find that the potential energy decays as $\approx r^{-3}$, suggesting the dipole-dipole interactions between Ir(ppy)$_3$ molecules. Furthermore, the repulsive interactions reflect the fact that each dipole moment is oriented in the same direction.

As indicated above, the appearance of three ppy ligands in the high-resolution STM image of Fig. 2(b) implies that the permanent dipole moment of Ir(ppy)$_3$ running along the C_3 axis is oriented perpendicular to the surface. In this case, two possible dipole directions, pointed toward the surface or the vacuum side, are expected, depending on whether the prydine or phenyl moieties of the ppy ligands are adsorbed on the surface. Since the adsorption directions are unable to be distinguished from the high-resolution STM images, we have performed the PM3 semiempirical molecular orbital calculations [22], in which 19 Cu atoms are included as a single surface layer of Cu(111) fixed with a bulk interatomic distance. From the geometry optimization, the stable adsorption structures have revealed that the three ppy ligands of Ir(ppy)$_3$ are adsorbed on the Cu surface without large deformation, and thus the C_3 symmetric axis is oriented perpendicular to the surface plane [as shown in Fig. 1(b)], which well reproduces the orientations and dimensions of the three protrusions appearing in the high-resolution STM images. Furthermore, when the prydine moieties of the ppy ligands are directly adsorbed on the Cu(111) surface, the calculated adsorption energy is 16.9 kcal/ mol lower than that for the opposite adsorbate direction. This large energy difference predicts that the dipole moments of nearly all adsorbed molecules are pointed toward the surface plane, on the basis of the Boltzmann distribution at a substrate temperature of 300 K during the molecular deposition. The direction selective adsorption of Ir(ppy)$_3$ should arise from the

anionic nature of the phenyl moieties preventing from the stable adsorption, compared with the neutral nature of the pyridine moieties.

The strong repulsive interactions of $Ir(ppy)_3$ should be originated from the direct dipole-dipole interactions, which are naïvely described as $E(r)_{\text{dipole}} = \mu^2/4\pi\epsilon_0 r^3$, where μ is the permanent dipole moment of $Ir(ppy)_3$. By fitting it to the experimental potential curve of Fig. 4 [23], we have obtained the dipole moment of adsorbed $Ir(ppy)_3$ molecules to be 9.18 ± 1.70 D, which is much larger than the calculation result of 6.5 D for intrinsic $Ir(ppy)_3$ [14]. This enhancement of the repulsive interactions should be explained by the effect of the mirror dipoles. The mirror dipoles are known to be produced inside of conducting surfaces [24], and due to the dipole-dipole and dipole-mirror dipole interactions as illustrated in the inset of Fig. 4, the potential is enhanced by a factor of 2. By including the influence of the mirror dipoles, the dipole moment is reevaluated to be 6.49 ± 1.20 D from the experimental potential curve, which is almost identical to that of $Ir(ppy)_3$. As a consequence, the surface-enhanced dipole-dipole interactions are dominated between $Ir(ppy)_3$ on the Cu(111) surface.

The strong and long-range repulsive intermolecular interactions will lead to the formation of highly dispersed superstructures with density-controlled intermolecular spacings, since the averaged separations are determined by the balance between the repulsion and dispersion interactions. As shown in Fig. 3, we observed almost uniformed molecular separations ranging from 1.7 nm to 3.6 nm in the superstructures, depending on the molecular density, although multilayer crystalline films were formed above a critical density of 0.24 nm^{-2}.

In conclusion, the surface-enhanced dipole-dipole interactions of adsorbed $Ir(ppy)_3$ molecules have been observed on the Cu(111) surface, as well as the indirect surface-mediated interactions. The repulsion is attributed to the orientation selective adsorption of dipolar $Ir(ppy)_3$ molecules on the Cu(111) surface, and it is enhanced by the effects of the mirror dipoles. The strong and long-range repulsive interactions lead to the formation of highly dispersed superstructures with density-controlled intermolecular spacings. In the superstructures, it should be noted that the dipole moment of all adsorbed molecules is oriented in the same direction (toward the surface), so that unusual electronic and optical properties are expected.

We thank Dr. M. Itoh for useful discussions. This work was in part supported by Grants in Aid from the Japanese Society for the Promotion of Science and by the Grant for Strategic Research Project of Yokohama City University.

*Author to whom correspondence should be addressed. Email address: tyoko@yokohama-cu.ac.jp

[1] C. Joachim, J. K. Gimzewski, and A. Aviram, Nature (London) **408**, 541 (2000).
[2] J. V. Barth, G. Costantini, and K. Kern, Nature (London) **437**, 671 (2005).
[3] M. Böhringer, K. Morgenstern, W.-D. Schneider, R. Berndt, F. Mauri, A. DeVita, and R. Car, Phys. Rev. Lett. **83**, 324 (1999).
[4] J. Weckesser, A. DeVita, J. V. Barth, C. Cai, and K. Kern, Phys. Rev. Lett. **87**, 096101 (2001).
[5] T. Yokoyama, S. Yokoyama, T. Kamikado, Y. Okuno, and S. Mashiko, Nature (London) **413**, 619 (2001).
[6] T. Yokoyama, T. Kamikado, S. Yokoyama, and S. Mashiko, J. Chem. Phys. **121**, 11 993 (2004).
[7] J.-M. Lehn, *Supramolecular Chemistry: Concept and Perspectives* (VCH, Weinheim, 1995).
[8] F. Silly, M. Pivetta, M. Ternes, F. Patthey, J. P. Pelz, and W.-D. Schneider, Phys. Rev. Lett. **92**, 016101 (2004).
[9] S. Lukas, G. Witte, and Ch. Wöll, Phys. Rev. Lett. **88**, 028301 (2001).
[10] E. Charles, H. Sykes, B. A. Mantooth, P. Han, Z. J. Donhauser, and P. S. Weiss, J. Am. Chem. Soc. **127**, 7255 (2005).
[11] A. Kiebele, D. Bonifazi, F. Cheng, M. Stöhr, F. Diederich, T. Jung, and H. Spillmann, Chem. Phys. Chem. **7**, 1462 (2006).
[12] K. A. King, P. J. Spellane, and R. J. Watts, J. Am. Chem. Soc. **107**, 1431 (1985).
[13] A. B. Tamayo, B. D. Alleyne, P. I. Djurovich, S. Lamansky, I. Tsyba, N. N. Ho, R. Bau, and M. E. Thompson, J. Am. Chem. Soc. **125**, 7377 (2003).
[14] J. Breu, P. Stössel, S. Schrader, A. Starukhin, W. J. Finkenzeller, and H. Yersin, Chem. Mater. **17**, 1745 (2005).
[15] M. A. Baldo, S. Lamansky, P. E. Burrows, M. E. Thompson, and S. R. Forrest, Appl. Phys. Lett. **75**, 4 (1999).
[16] Y. Sun, N. C. Giebink, H. Kanno, B. Ma, M. E. Thompson, and S. R. Forrest, Nature (London) **440**, 908 (2006).
[17] J. Repp, F. Moresco, G. Meyer, K.-H. Rieder, P. Hyldgaard, and M. Persson, Phys. Rev. Lett. **85**, 2981 (2000).
[18] N. Knorr, H. Brune, M. Epple, A. Hirstein, M. A. Schneider, and K. Kern, Phys. Rev. B **65**, 115420 (2002).
[19] P. Hyldgaard and M. Persson, J. Phys. Condens. Matter **12**, L13 (2000).
[20] The random separation distribution $f_{\text{ran}}(r)$ is expressed as $f_{\text{ran}}(r) = (2\pi r\Delta r N^2/L^2)(1 - \pi r^2/L^2)^N\{L^2 - (4rL - 4r^2) - \pi r^2\}/L^2$, where N is the number of molecules per image, L is the size of the image, and Δr is the width of the histogram classes [18].
[21] In order to avoid the influence of many-body interactions, we selected histograms obtained only at dilute densities.
[22] The quantum chemical calculations have been performed using the program package SPARTAN02 (Wavefunction, Inc., Irvine, CA).
[23] In the obtained potential, the surface Friedel oscillations $E_{\text{int}}(r)$ are also included, although the influence is negligible. Consequently, to evaluate the dipole moment, the fitting was performed after subtracting $E_{\text{int}}(r)$ from the experimentally obtained potential.
[24] E. M. McCash, *Surface Chemistry* (Oxford University Press, New York, 2001).